Effects of geometric and material nonlinearities on tunable band gaps and low-frequency directionality of phononic crystals

Effects of geometric and material nonlinearities on tunable band gaps and low-frequency directionality of phononic crystals

Pai Wang,[1] Jongmin Shim,[2] and Katia Bertoldi[1,3]
[1]*School of Engineering and Applied Sciences, Harvard University, Cambridge, Massachusetts 02138, USA*
[2]*Department of Civil, Structural and Environmental Engineering, University at Buffalo, Buffalo, New York 14260, USA*
[3]*Kavli Institute, Harvard University, Cambridge, Massachusetts 02138, USA*
(Received 4 March 2013; published 22 July 2013)

We investigate the effects of geometric and material nonlinearities introduced by deformation on the linear dynamic response of two-dimensional phononic crystals. Our analysis not only shows that deformation can be effectively used to tune the band gaps and the directionality of the propagating waves, but also reveals how geometric and material nonlinearities contribute to the tunable response of phononic crystals. Our numerical study provides a better understanding of the tunable response of phononic crystals and opens avenues for the design of systems with optimized properties and enhanced tunability.

DOI: 10.1103/PhysRevB.88.014304 PACS number(s): 63.20.dd, 43.35.+d, 62.30.+d

Phononic crystals (i.e., periodic structures composed of multiple materials with contrast in mechanical properties) have attracted considerable interest due to their ability to tailor the propagation of waves through band gaps, frequency ranges in which the propagation of sound and elastic waves is forbidden.[1–5] This fundamental property has been recently exploited to design waveguides,[6] frequency modulators,[7] noise-reduction devices,[8] and vibration isolators.[9] It has also been recognized that phononic crystals are characterized by directional behavior that can be exploited to steer or redirect waves in specific directions.[3,10,11] The directionality is determined by the level of anisotropy of the structure and can be fully controlled through proper arrangement of the material distribution at the unit cell level.[12] Furthermore, many previous studies have focused on the high frequency propagation directionality of phononic crystals,[13–15] while the strongly directional behavior in the low frequency/long wavelength regime is not fully explored despite important potential applications in broadband situations.[12]

Motivated by technological applications, a number of studies investigated the effects of both material properties (i.e., contrast in density, Young's modulus, and Poisson's ratio)[16,17] and geometry (i.e., volume fraction and topology)[18,19] on the characteristics of phononic crystals. However, in all these investigations the band gaps and the directionality of the propagating waves are limited to specific values that cannot be tuned after the manufacturing process. New strategies are required to design phononic crystals with adaptive properties that can be reversibly tuned.

It has been recently demonstrated that mechanical loading can be used as a robust mechanism for *in situ* tunability of soft and highly deformable two-dimensional phononic crystals.[5] It was shown that both the position and width of the band gap are strongly affected by the applied deformation.[5,20,21] However, the effect of deformation on the directionality of the propagating waves in the low frequency regime (i.e., the first longitudinal and shear modes) has never been studied. Finally, although it is evident that the applied deformation induces both strong geometric and material nonlinearities,[5] it is not clear how these two factors contribute to the tunability of the response. To shed light on these important points, here we investigate not only the effect of the applied deformation on the low frequency directionality of the propagating waves, but also the contributions of geometric and material nonlinearities to the tunable response of soft phononic crystals. The numerical analyses performed in this study offer a better understanding of the tunable response of phononic crystals and provide guidelines for the design of structures with optimized properties and enhanced tunability.

Here we focus on two-dimensional (2D) soft phononic crystals. Although our analysis is general and can be applied to any architecture, in this study we present numerical results for a square array of circular holes characterized by an initial void volume fraction $V_0 = 60\%$ [Fig. 1(a)]. Here V_0 is defined as the volume of the voids divided by the total volume of the phononic crystal. The nonlinear finite-element code ABAQUS/STANDARD is used to deform the structures as well as to investigate the propagation of small-amplitude elastic waves in the predeformed phononic crystal. Detailed description of the general formulation and the numerical simulations are provided in the Supplementary Materials.[22]

For all the analyses, 2D finite element models are constructed and the accuracy of the mesh is ascertained through a mesh refinement study. We focus on a phononic crystal made of an almost-incompressible elastomeric material whose response is captured by a Gent model[23] characterized by the following strain energy density function:

$$W(I_1, J) = -\frac{G}{2} J_m \log\left(\frac{J_m - (I_1 - 3)}{J_m}\right) - G\log(J) + \left(\frac{K}{2} - \frac{G}{J_m}\right)(J-1)^2, \quad (1)$$

where $I_1 = \mathrm{trace}(\mathbf{F}^T\mathbf{F})$, $J = \det(\mathbf{F})$, $\mathbf{F}$ denotes the deformation gradient, G and K are the initial shear and bulk moduli, and J_m denotes a material constant related to the strain at saturation. We note that the strain energy tends to infinity as $I_1 - 3$ approaches J_m.

Here we consider an elastomeric material with $G = 1.08 \times 10^6$ N/m^2, $K = 2.0 \times 10^9$ N/m^2 (Poissson's ratio $\nu = 0.4997$), and $\rho_0 = 1050$ kg/m^3, so that in the undeformed configuration the elastic wave speeds for shear and

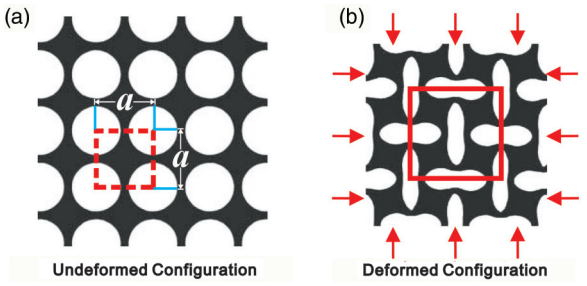

FIG. 1. (Color online) Geometry reorganization induced by instability in a soft phononic crystal comprising a square array of circular holes subjected to equibiaxial compression. The dashed square of size $a \times a$ in (a) indicates the primitive unit cell in the undeformed configuration. The solid square in (b) represents the enlarged representative volume element in the deformed configuration.

pressure waves in the material are $c_T = 32.07$ m/s and $c_L = 1381$ m/s, respectively. The effects of material nonlinearities are investigated by considering three different values of J_m, $J_m = 0.5, 2.0, \infty$. Note that, at the limit of $J_m \to \infty$, the strain energy density function (1) reduces to that of a Neo-Hookean material.[22,24] In Fig. 2 the material response under uniaxial loading is reported in terms of the nominal stress S, normalized by G, versus the uniaxial deformation stretch. The results clearly indicate that smaller values of J_m introduce stronger nonlinearities in the material behavior.

It is well known that, under compression, the geometric pattern of soft phononic crystals can suddenly change due to either: (a) microscopic instabilities with a spatial periodicity comparable to the size of the unit cell; or (b) macroscopic instabilities with a spatial periodicity much larger than the size of the unit cell.[25–28] Note that a detailed description of both micro- and macroscopic instabilities and the numerical procedure to calculate the onset of each case is provided in the Supplementary Materials.[22] In this study we investigate both instabilities of the phononic crystal under equibiaxial

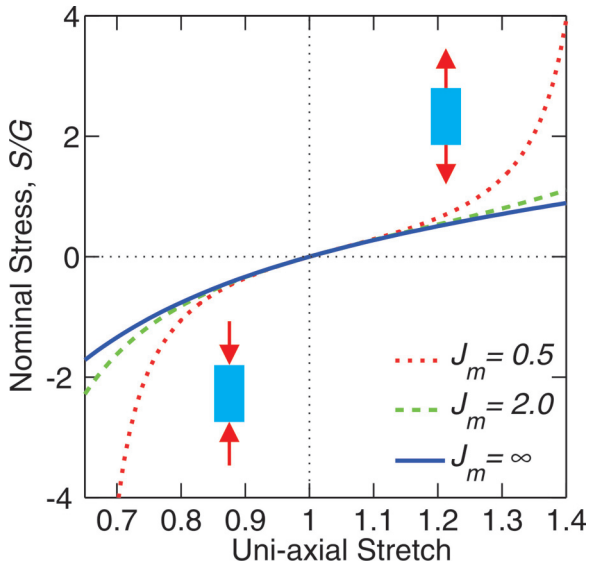

FIG. 2. (Color online) Uniaxial stress-stretch response of a nearly incompressible Gent material with $J_m = 0.5$, 2.0, and ∞ (the last corresponding to a Neo-Hookean material).

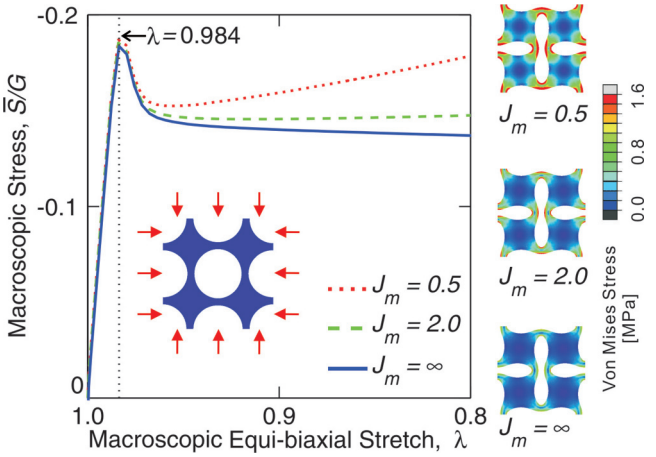

FIG. 3. (Color online) Macroscopic nominal stress vs stretch curves for the square array of circular holes in a Gent matrix. The departure from linearity is the result of an elastic instability that triggers the pattern transformation. The Von Mises stress distributions in the phononic crystals at $\lambda = 0.8$ are shown on the right for $J_m = 0.5$, 2.0, and ∞.

compression, so that the macroscopic deformation gradient $\bar{\mathbf{F}}$ is given by

$$\bar{\mathbf{F}} = \lambda(\mathbf{e}_1 \otimes \mathbf{e}_1 + \mathbf{e}_2 \otimes \mathbf{e}_2), \tag{2}$$

where λ denotes the macroscopically applied stretch and $\mathbf{e}_1$ and $\mathbf{e}_1$ are the basis vectors of two-dimensional Cartesian coordinates. We note that the undeformed configuration is characterized by $\lambda = 1$. Moreover, $\lambda > 1$ and $\lambda < 1$ represent the tension and compression load, respectively.

For the considered periodic structure, the onsets of both microscopic and macroscopic instabilities are detected by studying the response of a single unit cell [indicated by the dashed red square in Fig. 1(a)] along the loading path (2) by decreasing λ from unity. For all the cases considered here (i.e., $J_m = 0.5, 2.0, \infty$), a microscopic instability is detected at $\lambda_{\text{cr}}^{\text{Micro}} = 0.984$, while the onset of macroscopic instability occurs at $\lambda_{\text{cr}}^{\text{Macro}} = 0.961$. Therefore, microscopic instabilities are always critical in compression, leading to an enlarged representative volume element of 2×2 primitive unit cells and to the formation of a pattern of alternating, mutually orthogonal and elongated holes [Fig. 1(b)].

The postbuckling response of the phononic crystal is then simulated by introducing small random imperfections in the initial geometry.[22] In Fig. 3 we present the static response of the phononic crystal for the three considered values of J_m in terms of the macroscopically effective nominal stress $\bar{S}$ versus the applied stretch λ. Although the onset of instability is found not to be affected by J_m, we can clearly see that J_m has a strong influence on the postbuckling response of the structure.

To highlight the effect of the applied deformation on the propagation of elastic waves, we present in Fig. 4 the band structure and directionality diagrams of a phononic crystal made of a Gent material with $J_m = 0.5$ in both the undeformed [$\lambda = 1.0$, Fig. 4(a)] and deformed [$\lambda = 0.8$, Fig. 4(b)] configurations.

Figures 4(c) and 4(d) show the band diagrams of the undeformed and deformed configurations, respectively. The

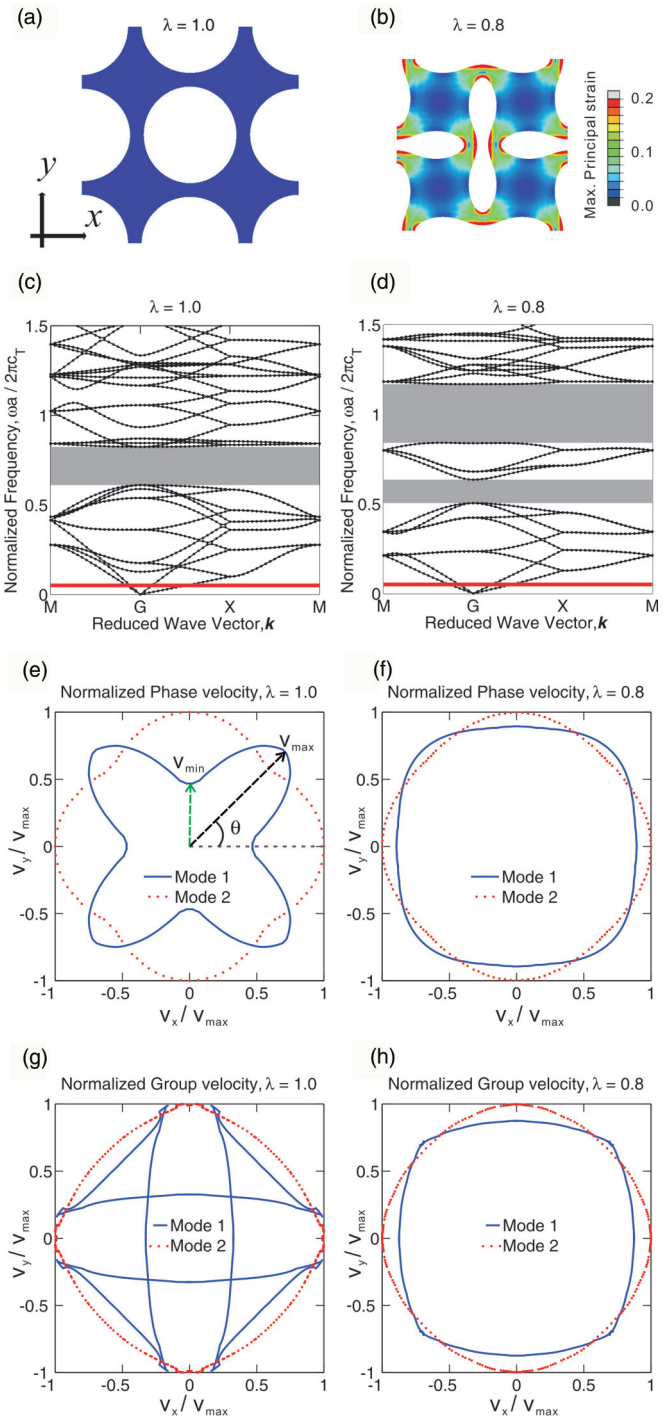

FIG. 4. (Color online) Dynamic response of the phononic crystal in the undeformed (left column, $\lambda = 1.0$) and deformed (right column, $\lambda = 0.8$) configuration. (c) and (d): effect of deformation on the band gaps. (e) and (f): effect of deformation on the directionality of phase velocities. (g) and (h): effect of deformation on the directionality of group velocities.

dimensionless frequency $\tilde{f} = \omega a/(2\pi c_T)$, with a denoting the characteristic size of the unit cell in the undeformed configuration [Fig. 1(a)], is plotted as a function of the wave vector in the reciprocal space.[22] In the undeformed configuration, the periodic structure features a band gap at $\tilde{f} = 0.61$–0.82. It is clear from Fig. 4(d) that the compression significantly alters the band structure. The pre-existing band gap is shifted and widened to $\tilde{f} = 0.84$–1.29. In addition, a new band gap that does not exist in the reference state is opened at $\tilde{f} = 0.50$–0.64.

To investigate the effect of deformation on the preferential directions of wave propagation, we focus on the low frequency range and calculate both phase velocity and group velocity for all directions of propagation at $\tilde{f} = 0.05$ [horizontal red line in Figs. 4(c) and 4(d)].[22] In Figs. 4(e) and 4(f) we report the phase velocity profiles and in Figs. 4(g) and 4(h) the group velocity profiles for the undeformed and deformed configurations, respectively. In these plots all the wave velocities are normalized, so that the magnitude of maximum velocity $v_{\max}$ of any mode in any configuration is unity. It is important to note that the wave directionality in the low frequency range cannot be fully captured just by inspecting the band diagrams.[12] In fact, although the dispersion curves at low frequency resemble straight lines, which seem to imply linear dispersion relations, the approximation of an effective nondispersive media is not applicable here, as phase and group velocities may exhibit very different directional behaviors.[12]

We start by noting that, in the undeformed configuration, the phase velocity shows a preferred direction of propagation at $\theta = 45^\circ$ for mode 1 (shear-dominated mode) and at $\theta = 0^\circ$ for mode 2 (pressure-dominated mode) [Fig. 4(e)]. Moreover, the group velocity in the undeformed configuration exhibits two preferred directions at $\theta = 10^\circ$ and 80° for mode 1 [Fig. 4(g)], whereas it does not show a significant preferential direction of propagation for mode 2. Finally, we note that the loped pattern in Fig. 4(g) entails two different group velocities in certain directions [a feature that cannot be directly observed in the standard dispersion relation in Fig. 4(c)]. In general, the group velocity, which is defined as the gradient of the dispersion surface,[22] can be at a different direction than the direction of the wave vector. Hence, two wave vectors of different directions may result in two group velocities of different magnitudes in the same direction.

In contrast, the deformed configuration does not exhibit any strong preference in directions for both phase and group velocities in both modes [Figs. 4(f) and 4(h)], so that it behaves as a nearly isotropic medium. These results clearly indicate that the deformation has a significant effect on the wave's directionality. Finally, we observe that the applied deformation has a more pronounced effect on the phase and group velocity profiles of mode 1 (shear-dominated mode), whereas the directionality of mode 2 (pressure-dominated mode) is only marginally affected.

The results presented above clearly show that the applied deformation strongly affects not only the static, but also the dynamic response of phononic crystals. However, to design the next generation of tunable phononic crystals that take full advantage of the changes on the dynamic response induced by the applied deformation, this mechanism needs to be thoroughly understood. While it is well known that the applied deformation introduces both geometric and material nonlinearities, it is not clear how these two effects control the tunable dynamic response of the phononic crystal. To gain knowledge on this front, we numerically investigate the separate effects of geometric and material nonlinearities on both the band gaps and wave directionality.

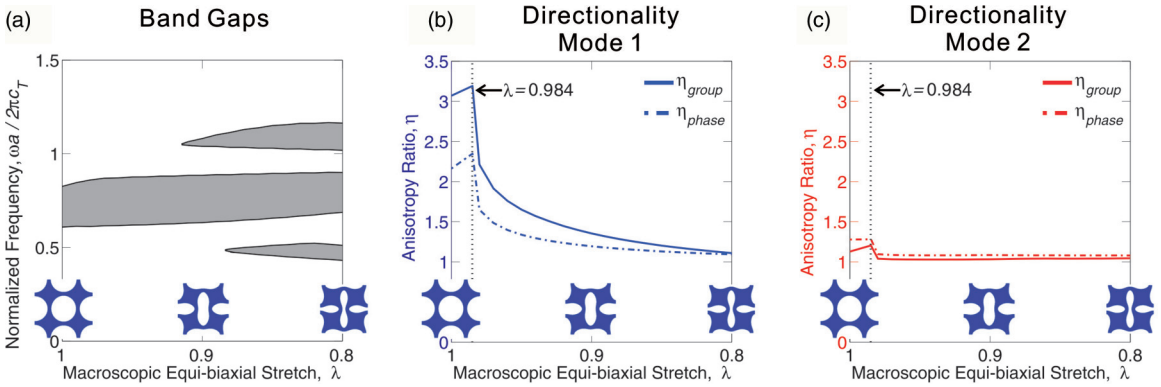

FIG. 5. (Color online) Effects of geometric nonlinearities on (a) band gaps and directionality of (b) mode 1 and (c) mode 2.

Geometric nonlinearities. To evaluate the effect of geometric nonlinearities on the dynamic response of the phononic crystal, we investigate the propagation of elastic waves in a stress-free structure with the deformed geometry (i.e., the shape of the structure is determined by the postbuckling analysis). More specifically, we compress the structure up to a certain value of λ and then set the all the components of the stress to zero before performing the wave propagation analysis. Thus, the inhomogeneous stress distribution is not taken into the consideration when computing the dynamic response.

The evolution of the band gaps as a function of λ is shown in Fig. 5(a). The change in geometry induced by the applied deformation is found to shift and widen the main band gap and to generate two additional band gaps, one higher and the other lower than the main gap, which open at $\lambda = 0.92$ and $\lambda = 0.88$, respectively. These deformation-induced band gaps also shift and widen for decreasing values of λ. Finally, we note that these results are independent of J_m since in order to investigate the geometric effects alone, we have neglected the stress distribution in the deformed configuration (note that the incremental response for an unstressed Gent material is independent of J_m).

To describe the evolution of the directionality of propagating waves, we define the anisotropy ratio:

$$\eta = \frac{v_{\max}}{v_{\min}}, \tag{3}$$

where $v_{\max}$ and $v_{\min}$ are the maximum and minimum wave velocities, respectively [see Fig. 4(e)]. The trends of η for both phase velocity and group velocity of mode 1 (shear-dominated mode) and mode 2 (pressure-dominated mode) as a function of λ are reported in Figs. 5(b) and 5(c), respectively.

For mode 1, the anisotropy ratios of both the group and phase velocity profiles (η_{group} and η_{phase}) rise from the initial values up to a turning point, then rapidly decrease as a function of λ and approach unity [Fig. 5(b)]. Note that the turning point at $\lambda = 0.984$ corresponds to the onset of structural instability. Similar trends are observed for mode 2 [Fig. 5(c)], but the changes induced by deformation are less dramatic in this case. In summary, the results from both modes show that the geometric nonlinearities induced by instability have a significant effect on the wave directionality. They remove the directional characteristics of both modes and make the wave propagation more isotropic.

Material nonlinearities. It is apparent from Fig. 4(b) that deformation not only affects the geometry, but also induces an inhomogeneous strain/stress distribution within the phononic crystal. Substantial stress concentrations are developed during compression and they strongly depend on the nonlinear material response, which is characterized by J_m (Fig. 3).

To investigate the effect of material nonlinearities on the propagation of elastic waves, we start by studying the response of a phononic crystal made of a Neo-Hookean material (i.e., Gent material with $J_m = \infty$). The response of such material is weakly nonlinear and the stiffening effect induced by the applied deformation is negligible in this case. In Fig. 6(a) we report the evolution of the band gaps as a function of the

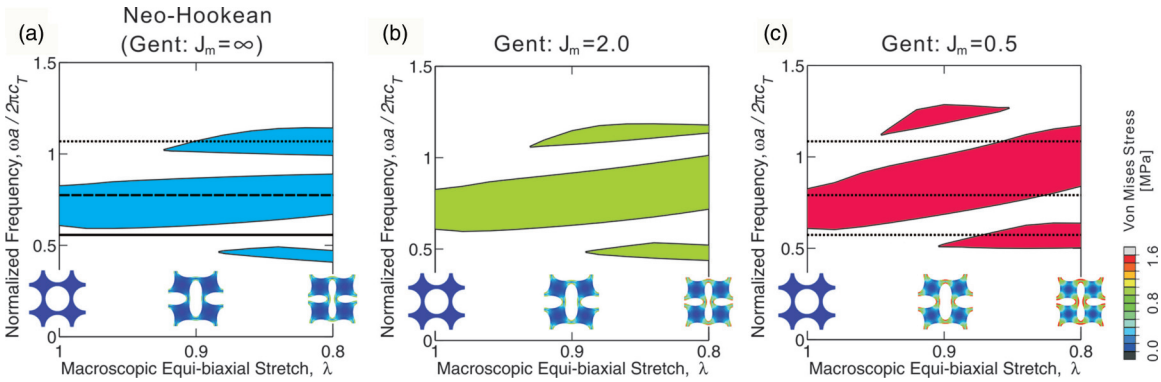

FIG. 6. (Color online) Effects of material nonlinearities on the band gaps. Soft phononic crystals made of Gent materials with (a) $J_m = \infty$, (b) $J_m = 2.0$, and (c) $J_m = 0.5$ are investigated.

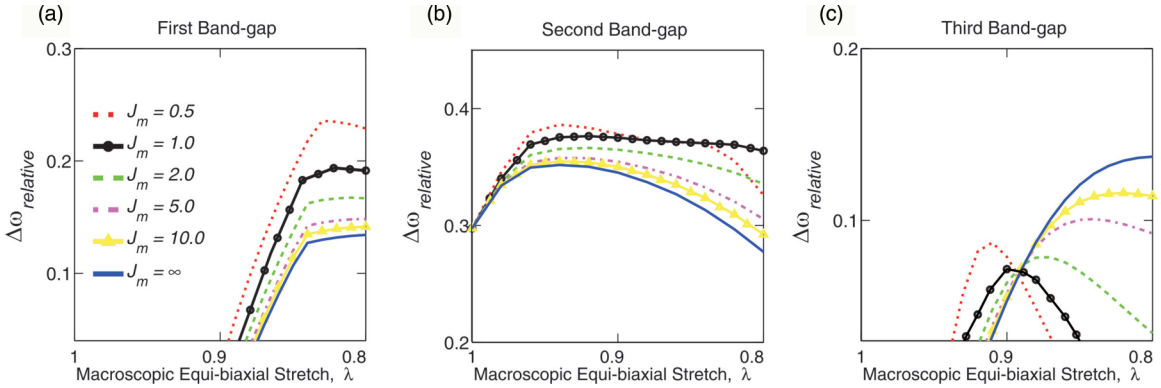

FIG. 7. (Color online) Comparison of the change of relative band gaps during deformation.

applied deformation λ. Comparison between Figs. 5(a) and 6(a) reveals that the dynamic response of the phononic crystal is not affected by the inhomogeneous stress state. Therefore, for a phononic crystal made of an Neo-Hookean elastomeric material, the geometric nonlinearities induced by the applied deformation fully control the position and width of the band gaps.

Next, we investigate the evolution of the band gaps for phononic crystals made of elastomers with stronger material nonlinearity. As shown in Fig. 2, smaller values of J_m introduce stronger material nonlinearities under the applied deformation. Here we comparatively study the cases of phononic crystals made of Gent materials with $J_m = 2.0$ and 0.5 [Figs. 6(b) and 6(c)]. We notice that in both cases the band gaps are significantly affected by material nonlinearities when $\lambda < 0.9$. We find that smaller values of J_m provide a larger range of tunability for the band gaps. To better quantify the effect of material nonlinearity on the band gap tunability, we divide the wave frequencies into three categories: (i) frequencies that are always in the propagating band [e.g., $\tilde{f} = 0.55$, continuous horizontal line in Fig. 6(a)]; (ii) frequencies that are always in the band gap [e.g., $\tilde{f} = 0.75$, dashed horizontal line in Fig. 6(a)]; and (iii) frequencies that can be switched on/off by the applied deformation [e.g., $\tilde{f} = 1.05$, dotted horizontal line in Fig. 6(a)]. We start by noting that all the three frequencies highlighted in Fig. 6(a) turn into category (iii) when $J_m = 0.5$ [see dotted horizontal lines in Fig. 6(c)]. In fact, for $J_m = 0.5$, the frequencies in the entire region $\tilde{f} =$ 0.49–1.28 can be switched on/off by the applied deformation. Therefore, since large regions of type (iii) frequencies are desirable for the design of a highly tunable system, our results indicate that phononic crystals made of materials with stronger nonlinearities can offer enhanced band gap tunability.

In addition, our analysis also reveals that material nonlinearities do not affect the directionality of the propagating waves at low frequency. The velocity profiles obtained for phononic crystals made of Gent material with $J_m = \infty$, 2.0, and 0.5 are found to be the same as those shown in Figs. 5(b) and 5(c). The same behavior is also observed for the case of triangular and trihexagonal arrays of circular holes (see Supplementary Materials),[22] suggesting that only changes in geometry can be effectively used to tune the directional characteristics of the lower bands. This is due to the fact that the wavelength of the low frequency propagating modes are very long compared with the length scale of the local variations of stress field.

To further study the effect of the material parameter J_m on the band gaps, we calculate the relative size of the band gaps as the ratio between gap width and the midgap position,

$$\Delta\omega_{\text{relative}} = \frac{\omega_{\text{upper}} - \omega_{\text{lower}}}{(\omega_{\text{upper}} + \omega_{\text{lower}})/2}, \tag{4}$$

where ω_{upper} and ω_{lower} are the frequencies of upper and lower edge limits of a band gap, respectively. It has been previously shown that the relative size defined above is a important design parameter, and that a large relative size of the band gap is preferable for many applications.[4] The evolution of $\Delta\omega_{\text{relative}}$ as a function of the applied deformation is reported in Figs. 7(a)–7(c) for the first, second, and third band gap, respectively. The responses of phononic crystals made of Gent material with $J_m = 0.5$, 1.0, 2.0, 5.0, 10.0, and ∞ are considered. For all different materials considered here and for all three band gaps $\Delta\omega_{\text{relative}}$ is found first to increase as a function of the applied deformation, then to reach a maximum and finally either to plateau or slightly decrease. For instance, in the case of $J_m = 0.5$, $\Delta\omega_{\text{relative}}$ reaches the maximum value at $\lambda = 0.83$, 0.94, and 0.91 for the first, second, and third band gaps, respectively. We note that the decrease of $\Delta\omega_{\text{relative}}$ after its maximum is due to the fact that the position shifting effect is stronger than the widening effect. That is, in Eq. (4), the increase in the denominator becomes faster than the increase in the numerator. As a result, although the band gap keeps widening upon further deformation, $\Delta\omega_{\text{relative}}$ diminishes. This feature described above becomes more pronounced when the applied deformation is large and the constituting material is highly nonlinear.

To summarize, we use numerical simulations to study the propagation of small-amplitude elastic waves in highly deformed phononic crystals and investigate the effect of deformation on band gaps and directionality of propagating waves. The contributions of geometric and material nonlinearities to the tunable response of phononic crystals are revealed. The band gaps are found to be affected both by geometric and material nonlinearities, while the directional preferences of the wave modes in the first two bands are shown to be sensitive only to changes in geometry. Enhanced tunability of the band gaps is found for phononic crystals made of materials with

stronger nonlinear behavior. Finally, the changes in geometry introduced by the applied deformation gradually remove the directional characteristics of the lowest two propagation modes, making the wave propagation more isotropic. The results presented in this paper provide useful guidelines for the design of tunable phononic devices.

This work has been supported by Harvard MRSEC through Grant No. DMR-0820484 and by NSF through Grants No. CMMI-1120724 and No. CMMI-1149456 (CAREER). K.B. acknowledges start-up funds from the Harvard School of Engineering and Applied Sciences and the support of the Kavli Institute and Wyss Institute at Harvard University.

[1] M. Sigalas and E. Economou, Solid State Commun. **86**, 141 (1993).
[2] M. S. Kushwaha, P. Halevi, L. Dobrzynski, and B. Djafari-Rouhani, Phys. Rev. Lett. **71**, 2022 (1993).
[3] M. Ruzzene and F. Scarpa, Phys. Status Solidi B **242**, 665 (2005).
[4] M. Maldovan and E. Thomas, Appl. Phys. B **83**, 595 (2006).
[5] K. Bertoldi and M. C. Boyce, Phys. Rev. B **78**, 184107 (2008).
[6] J. O. Vasseur, A. Hennion, B. Rouhani, F. Duval, B. Dubus, and Y. Pennec, J. App. Phys. **101**, 114904 (2007).
[7] W. Cheng, J. J. Wang, U. Jonas, G. Fytas, and N. Stefanou, Nat. Mater. **5**, 830 (2006).
[8] F. Casadei, L. Dozio, M. Ruzzene, and K. Cunefare, J. Sound. Vib. **329**, 3632 (2010).
[9] F. Casadei, B. Beck, K. A. Cunefare, and M. Ruzzene, J. Intel. Mat. Syst. Str. **23**, 1169 (2012).
[10] M. Ruzzene, F. Scarpa, and F. Soranna, Smart. Mater. Struct. **12**, 363 (2003).
[11] M. Collet, M. Ouisse, M. Ruzzene, and M. N. Ichchou, Int. J. Solids Struct. **48**, 2837 (2011).
[12] F. Casadei and J. J. Rimoli, Int. J. Solids Struct. **50**, 1402 (2013).
[13] E. Nolde, R. Craster, and J. Kaplunov, J. Mech. Phys. Solids **59**, 651 (2011).
[14] S. Gonella and M. Ruzzene, Int. J. Solids Struct. **45**, 2897 (2008).
[15] S. Gonella and M. Ruzzene, J. Sound Vib. **312**, 125 (2008).
[16] J. O. Vasseur, B. Djafari-Rouhani, L. Dobrzynski, M. S. Kushwaha, and P. Halevi, J. Phys. Condens. Mater. **6**, 8759 (1994).
[17] X. Zhou, Y. Wang, and C. Zhang, J. Appl. Phys. **106**, 014903 (2009).
[18] A. B. Movchan, N. V. Movchan, and S. Haq, Mater. Sci. Eng. **431**, 175 (2006).
[19] M. Maldovan and E. Thomas, *Periodic Materials and Interference Lithography for Photonics, Phononics and Mechanics* (Wiley-VCH, Berlin, 2009).
[20] J. Jang, C. Koh, K. Bertoldi, M. Boyce, and E. Thomas, Nano Lett. **9**, 2113 (2009).
[21] L. Wang and K. Bertoldi, Int. J. Solids Struct. **49**, 2881 (2012).
[22] See Supplemental Material at http://link.aps.org/supplemental/10.1103/PhysRevB.88.014304 for the details of the general formulation and numerical procedures.
[23] A. Gent, Rubber Chem. Tech. **69**, 59 (1996).
[24] L. Treloar, Trans. Faraday Soc. **40**, 59 (1944).
[25] G. Geymonat, S. Muller, and N. Triantafyllidis, Arch. Ration. Mech. Anal. **122**, 231 (1993).
[26] N. Triantafyllidis, M. D. Nestorovic, and M. W. Schraad, J. Appl. Mech. **73**, 505 (2006).
[27] K. Bertoldi, M. Boyce, S. Deschanel, S. M. Prange, and T. Mullin., J. Mech. Phys. Solids **56**, 2642 (2008).
[28] Overvelde, S. Shan, and K. Bertoldi, Adv. Mater. **24**, 2337 (2012).